European Journal of Mechanics / B Fluids 74 (2019) 260–264

Contents lists available at ScienceDirect

European Journal of Mechanics / B Fluids

journal homepage: www.elsevier.com/locate/ejmflu

# Measuring surface gravity waves using a Kinect sensor

Francesco Toselli *, Filippo De Lillo, Miguel Onorato, Guido Boffetta

*Dipartimento di Fisica, Università di Torino and INFN, Sezione di Torino, Via P. Giuria, 1 - Torino, 10125, Italy*

ARTICLE INFO

*Article history:*
Received 13 June 2018
Received in revised form 9 August 2018
Accepted 29 August 2018
Available online 31 August 2018

*Keywords:*
Surface gravity wave
Space–time measurements
Dispersion relation

ABSTRACT

We present a technique for measuring the two-dimensional surface water wave elevation both in space and time based on the low-cost Microsoft Kinect sensor. We discuss the capabilities of the system and a method for its calibration. We illustrate the application of the Kinect to an experiment in a small wave tank. A detailed comparison with standard capacitive wave gauges is also performed. Spectral analysis of a random-forced wave field is used to obtain the dispersion relation of water waves, demonstrating the potentialities of the setup for the investigation of the statistical properties of surface waves.


## 1. Introduction

Surface gravity waves are waves that propagate on the interface between two fluids, for example air and water, in the presence of a gravitational force that acts as a restoring force. One of the most common examples is given by ocean waves that can propagate for hundreds of kilometers, after being generated and forced by the wind. Their dynamics is ruled by the Navier–Stokes equations; however, due to the complexity of such equations one usually relies on simplified models or on experiments. Traditionally, the displacement of the free surface from its equilibrium position has been measured using buoys (see for example [1,2]) and capacitive or resistive wave gauges. The former are commonly used in the field, the latter are usually adopted in more controllable environments because of their fragility, even though measurements in open seas have been performed (see for example [3] or more recently [4]). In the pioneering work of [5], a method for estimating the directional spectra from buoys has been given: the idea relies on the measurement not only of the vertical acceleration of a buoy but also of the angle of roll and pitch. Using these observables one can extract a limited number of Fourier coefficients of the angular distribution of the energy in each frequency band, reconstructing an energy spectrum as a function of frequency and angle of propagation of the waves. Despite the extremely important role played by such measurements for the understanding of many properties of ocean surface gravity waves (including spectra and other statistical quantities), these techniques are not satisfactory if one is interested in addressing the problem of the dynamics of surface waves. Indeed, starting from the late fifties (see [6]), optical techniques have been developed for application to ocean waves. Images of the surface elevation provide the spatial properties of the waves and can be used to compute wave number spectra as in [7,8] where an airborne scanning lidar system as been developed to measure spatially ocean waves. However, to study the wave dynamics, surface elevation needs to be measured both in space and time A recent important development in this direction has been provided by stereographic recordings of ocean waves (see [9–11]). Such measurement techniques allow one to reconstruct the dispersion relation of water waves, [12]. Optical methods based on profilometry [13,14] have also been developed to measure the 2D surface elevation in space and time and extract different regimes of wave turbulence in small scale experiments.

We present here a high resolution method for measuring the 2D elevation field of water waves based on the Microsoft Kinect depth sensor. We show that Kinect is able to reconstruct with good accuracy the time dependent configuration of surface wave of moderate amplitude and is a therefore a low-cost device for studying water wave dynamics in the laboratory. The remaining of this paper is organized as follows. Section 2 is devoted to the discussion of the hardware and the software and the calibration procedure. In Section 3 we discuss the results of the measures performed on water waves produced in a laboratory setup. The pointwise wave height measured with the Kinect is compared with measurements obtained by capacitive probes and the wave-fields obtained with the Kinect are used to reconstruct the dispersion relation of gravity waves. Finally, in Section 4 conclusions and perspectives will be discussed.

## 2. Methods

The core of the acquisition system is the Kinect sensor (Windows edition) [15], which includes a depth sensor based on infrared (IR) imaging, originally developed by Microsoft as a motion

* Corresponding author.
*E-mail address:* francesco.toselli@unito.it (F. Toselli).

https://doi.org/10.1016/j.euromechflu.2018.08.017
0997-7546/

sensing device for videogames. Producing data similar to a light detection and ranging sensor, the Kinect has the advantage to be cheaper and smaller than other tools commonly used to assimilate this kind of data. These characteristics make it a good candidate for practical use in providing high-level precision measurements in Earth science studies such as water waves amplitude reconstruction, and free-surface flow and bathymetry measurements [16].

### 2.1. Hardware

The Kinect sensor contains an IR emitter coupled with an IR depth sensor camera and range images are produced from the so-called light coding technique. The IR emitter generates a pattern on the observed object. The object needs to be opaque in order to diffuse the projected pattern which will be captured by the IR sensor. The image received by the sensor is compared with the original pattern by an on-board processor which uses the relative distortion to associate depth information to each pixel. The Kinect returns the depth field with a spatial resolution of $640 \times 480$ pixels and 11-bit depth quantization. It operates with a refresh rate of 30 Hz and, depending on the recording mode chosen, it can be used in a "default" (nominal optimal depth range between 1–6 m) or a "near" mode (0.5–3 m). In studying the capability of the sensor to detect wave amplitudes, we found an optimal working distance between 700 mm and 800 mm using the device in near mode. In this range the horizontal/vertical and depth resolutions of the sensor is around 1–2 mm [17]. The Kinect IR camera has a nominal field of view (FoV) of about $58 \times 45$ degrees, therefore the dimension of the recorded region placed at 750 mm from the sensor is about $800 \times 600$ mm$^2$.

Together with the depth sensor, the Kinect is equipped with an RGB camera at resolution $1280 \times 960$ pixels that can record simultaneously with the IR sensor and it is therefore useful to check the area of investigation; a 4-microphone array and an on-board accelerometer, that in the absence of linear accelerations, can be used for establishing the device orientation in space by measuring angles, are also part of the Kinect. The simultaneous use of the RGB and IR cameras requires specific calibration in order to obtain the correct correspondence between the respective FoV. However, we did not use the RGB sensor, instead inferring all geometrical information from the IR camera.

### 2.2. Software

The software interface was composed by a first module that acquires the data from the sensor and stores it on disk and a post-processing module that performs the actual wave detection. The first module, implemented in C#, leverages the Microsoft API (Kinect for Windows SDK 2.0) to interact with the device driver, and includes a graphical interface to help position the sensor. Afterwards the sensor data is stored as an image in the PNG format, enabling loss-less compression and high channel depth (in our case, 16 bit).

### 2.3. Calibration of the sensor

The calibration of the sensor was performed in several steps, using a plastic plane as a reference flat surface. The plane was positioned horizontally with a digital level with a precision of 0.1°. The sensor was installed over the plane in horizontal position (using the digital level) on a 3-axis camera mount and the values of the internal accelerometer (resolution 0.1 g) recorded for future alignment on the water wave tank.

We measured the noise level of the depth signal when viewing a flat surface at fixed distance. Time sequences of 90 images were acquired and the standard deviation $\sigma_d$ of the depth of each pixel

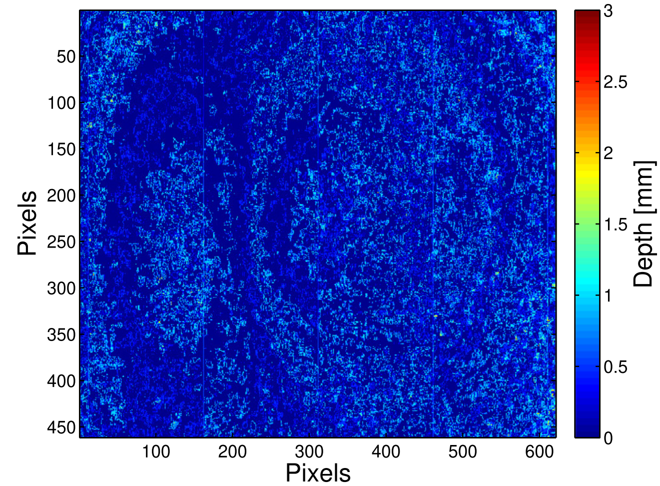


**Fig. 1.** Two-dimensional standard deviation map computed by using 3 s of record from a flat fixed surface. In most of the pixels the standard deviation is of the order of the nominal vertical sensibility of 1 mm.

was computed. The resulting map of standard deviations is shown in Fig. 1. For most of the pixels $\sigma_d$ is lower than the nominal vertical resolution of 1 mm.

We have then calibrated the depth sensor by collecting data for a flat surface placed at 11 different known distances from the sensor in the range 600–900 mm. For each distance one minute of data (1800 images) are acquired and these depth fields are averaged together to eliminate noise. For each pixel $(px, py)$ of the averaged image we use a linear model to connect the depth value $pz$ to the physical distance $z$ as

$$z = m(px, py)pz + q(px, py) \tag{1}$$

which defines the two matrices of coefficients $m(px, py)$ and $q(px, py)$. We found that the linear model works very well with global regression coefficient $R = 0.998$. We remark that the model expressed by (1) neglects possible aberrations due to the lens. This assumption was verified by systematically analyzing the position of the digital image of objects of known physical position (spanning both the horizontal and vertical ranges of the instrument), which gave no measurable distortion within the resolution of the depth sensor.

### 2.4. Experimental setup

In order to verify the possibility to measure the dynamic evolution of a surface-wave field, we placed the sensor over a wave tank and performed recordings of the evolving surface. Fig. 2 shows a schematic representation of the setup. We use a small linear wave tank, of horizontal sizes 2000 mm $\times$ 500 mm and depth 250 mm.

A wave generator was placed on the short side. No absorber was used on the opposite side, allowing for standing waves. The wave generator consists of a wedge fixed to a vertical motorized linear guide. The wedge moves between two switches which invert the linear motor. The motion of the wedge in the water forces waves whose amplitude and frequency is controlled via the positions of the switches (changing the depth of immersion) and the speed of the linear motor.

The Kinect sensor cannot detect the surface of pure water because of its transparency. For this reason the tank was filled with about 18 cm of water with the addition of white liquid dye (1% in volume of commercial paint soluble in water). This method allowed to make the liquid opaque and detect the water surface [18].

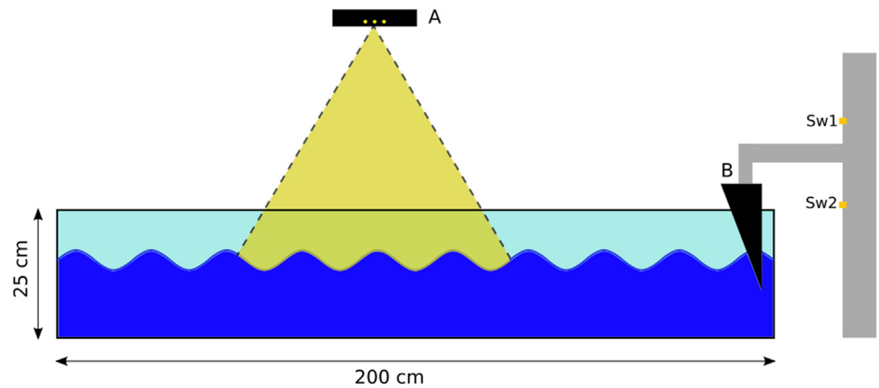


**Fig. 2.** Scheme of the experimental setup (not in scale). The FoV of the sensor A is positioned several wavelengths away from the wavemaker in order to avoid spurious fronts coming from the wedge B. The linear motor inverts the motion of the wedge when it reaches one of the switches Sw1 and Sw2.

The Kinect was installed on the 3-axis camera mount used for the calibration at a distance of about 75 cm from the fluid surface. The orientation of the sensor was set consistently with the calibration setup using as reference the readings of the internal accelerometer.

Kinect acquisitions were complemented with local measurements of surface height, obtained with a wave gauge system (INSEAN, Rome) consisting of two capacitive probes read by an interface which digitizes the signal and connects with a personal computer. The system has a sensitivity of 1 mm and the probes were placed inside the tank just outside the Kinect FoV, in order not to interfere with the acquired images.

## 3. Results

By changing the amplitude and the frequency of the wave forcing, we test the potentiality of our setup for the analysis of wave fields of amplitude between 2 and 20 mm.

At each time frame the sensor outputs a 2D image where the amplitude of each pixel gives the distance of the corresponding point in space from the device. Apart from the intrinsic noise in the measure, some limitations are specific to this method of measurement. Of particular relevance for experimental fluid mechanics is the presence of some reflection of the liquid surface. Indeed, in order for the device to correctly infer the distance of surfaces, a clean, purely diffusive image of the projected pattern must reach the IR sensor. As a consequence, the Kinect is unable to provide depth data for some pixels (see Fig. 3) due to direct reflection of the IR pattern at small angles. In our case we could verify that very few pixels suffered from these artifacts. Straightforward post-processing was used in order to replace the missing pixels by interpolating the surrounding valid pixels (see panel (b) in Fig. 3).

In order to estimate the reliability of the wave height data obtained with the Kinect, we compared it with the measurements from capacitive probes. Here we show two different time series with the same wave forcing period (1.1 s) but different amplitudes.

For this comparison we placed the capacitive probe at the center of the tank, one centimeter out of the FoV and upstream from it. The depth measured with the wave gauge was compared with the Kinect output averaged over a line transverse to the wave motion approximately 1.2 cm inside the FoV and directly downstream from the capacity probe. As one can see from Fig. 4 we found a good agreement between amplitude values referred to the two different kind of acquisition: even water waves with small amplitudes (panel (b) in Fig. 4), although presenting a bigger noise, are well captured and represented by the device.

Finally, as a proof of concept, we attempted to reconstruct the dispersion relation of the recorded wave field. We explored the sensor's capabilities to reconstruct the dispersion relation connecting the wave number $k$ of water waves with their angular frequency $\omega$. According to the linear theory, for arbitrary water depth $h$, such relation is:

$$\omega = \sqrt{g\,k\,\tanh(kh)}, \tag{2}$$

where $g$ is the gravity acceleration and $k$ is the wave number.

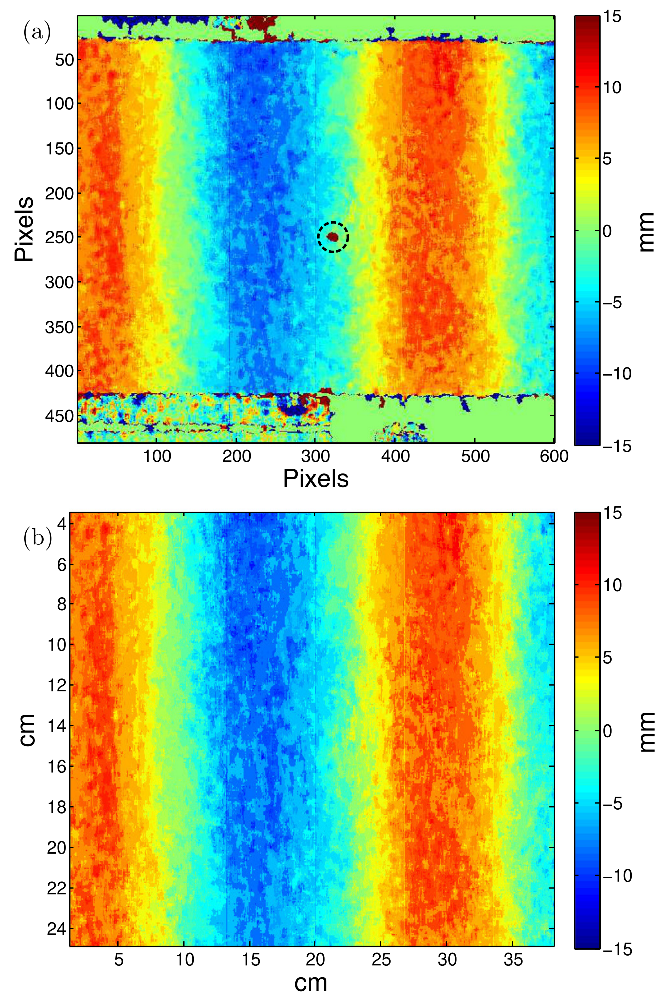


**Fig. 3.** Depth field before and after post processing. (a) Original Kinect depth data: regions outside the tank can be identified, as well as a limited number of pixels in the region inside the dashed black circle corresponding to the central area of the FoV where direct reflection produces spurious distances. (b) Depth data after cropping and removing reflective spots with interpolation.

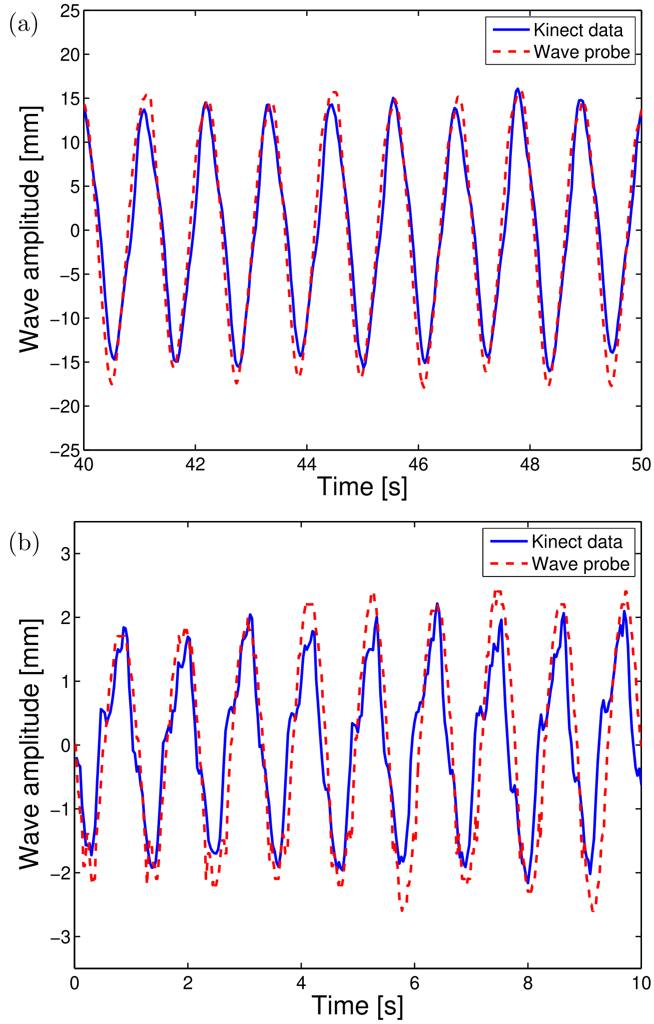


**Fig. 4.** Time series of the depth signal averaged over a line of pixels at the same longitudinal position, near (and parallel to) the edge of the FoV closest to the wave-maker. Panels (a) and (b) were obtained with the same forcing frequency and different amplitude. The Kinect data (solid line) are compared with the measurements from a capacitive probe (dashed line) a few centimeters away, just outside the Kinect sensor FoV. The signal for the smaller wave (b) is clearly more noisy, but it is for both instruments and still shows good agreement between the two methods.

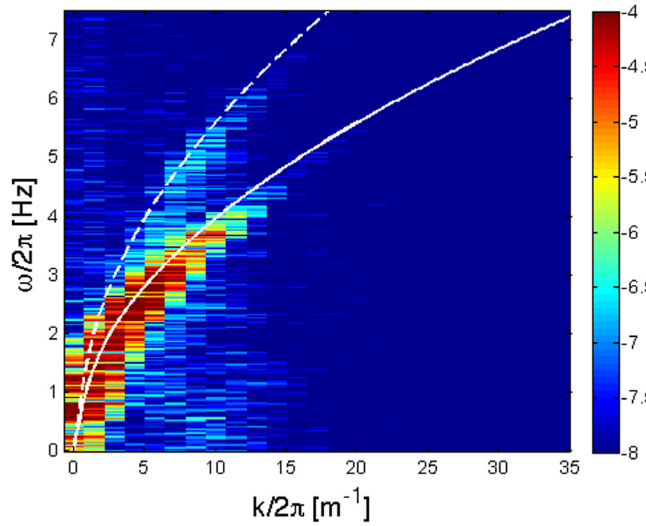


**Fig. 5.** Image of space–time Fourier wave spectrum computed on Kinect post processed data. The continuous line represents the relation between wave number $k$ and angular frequency $\omega$ given by the theoretical dispersion law, while the dashed line is its second harmonic. Energy is color coded on a logarithmic scale.

Clearly this relation requires data points at several frequencies. For this analysis we injected energy in the tank with a random forcing and we performed a two dimensional space–time Fourier transform of the wave fields. We expect the propagation of linear gravity waves to produce intense peaks in the Fourier transform corresponding to the $k$-$\omega$ pairs satisfying relation (2).

As one can see from Fig. 5, we found a high correlation between the theoretical dispersion relation and the collocation in $(k, \omega)$ Fourier space of the most energetic modes.

## 4. Conclusions

We presented some results on the use for scientific purposes of a commodity depth sensor, the Microsoft Kinect, originally designed for videogames use. The particular application we proposed is the laboratory measurement of surface water waves. Other uses of the same sensor have been proposed, among which the automatic analysis of crowds [19]. For such application the accuracy of the depth measurement is less critical since the sensor is used to provide data which can be fed to shape recognition software. For the measurement of water waves, the main drawback is the necessity to render the water opaque. While we showed that this can be done rather inexpensively using water-soluble paint, further characterization of the solution is needed in order to clarify the rheological effects of the specific substance employed. Our results show that the Kinect can be effectively used for the analysis of waves with amplitudes exceeding a few millimeters, wavelengths between 5 and 40 cm and frequencies up to 6 Hz, and it is therefore suitable for studies in the laboratory. Our setup allowed us to measure the dispersion relation of surface waves, thus serving as a proof of concept for the use of the device for non-trivial, multi-frequency statistical analysis of a wave-field. All post-processing used in our analysis can be easily automated, thus making for a cost-effective detector for surface waves. Further development in the post-processing package can potentially increase the vertical resolution by optimized noise reduction.

## Acknowledgments

Experiments were supported by the European Community Framework Program 7, European High Performance Infrastructures in Turbulence (EuHIT), Italy, Contract No. 312778. Support from the "Departments of Excellence" (L. 232/2016) grant, funded by the Italian Ministry of Education, University and Research (MIUR), Italy, is acknowledged. M.O. has been funded by Progetto di Ricerca d'Ateneo, Italy, CSTO160004. We thank A. Corbetta and F. Toschi for help in developing the software interface for Kinect.

## References

[1] Ocean Wave Spectra: Proceedings of a Conference Sponsored by the U.S. Naval Oceanographic Office and the Division of Earth Sciences, National Academy of Sciences, National Research Council, Prentice Hall, 1963.
[2] B. Kinsman, Wind Waves: Their Generation and Propagation on the Ocean Surface, Courier Corporation, 1965.
[3] L. Cavaleri, S. Zecchetto, Reynolds stresses under wind waves, J. Geophys. Res. C Oceans 92 (C4) (1987) 3894–3904.
[4] D.T. Resio, C.E. Long, C.L. Vincent, Equilibrium-range constant in wind-generated wave spectra, J. Geophys. Res. C Oceans 109 (2004) C01018.
[5] Michael S. Longuet-Higgins, D.E. Cartwright, N.D. Smith, Observations of the directional spectrum of sea waves using the motions of a floating buoy, in: Ocean Wave Spectra: Proceedings of a Conference, in: Ocean Wave Spectra, Prentice-Hall, 1963, pp. 111–136.

[6] C.S. Cox, Measurements of slopes of high-frequency wind waves, J. Mar. Res. 16 (1958) 199–225.
[7] P.A. Hwang, D.W. Wang, E.J. Walsh, W.B. Krabill, R.N. Swift, Airborne measurements of the wavenumber spectra of ocean surface waves. Part I: Spectral slope and dimensionless spectral coefficient, J. Phys. Oceanogr. 30 (11) (2000) 2753–2767.
[8] P.A. Hwang, D.W. Wang, E.J. Walsh, W.B. Krabill, R.N. Swift, Airborne measurements of the wavenumber spectra of ocean surface waves. Part II: Directional distribution, J. Phys. Oceanogr. 30 (11) (2000) 2768–2787.
[9] A. Benetazzo, Measurements of short water waves using stereo matched image sequences, Coastal Eng. 53 (12) (2006) 1013–1032.
[10] A. Benetazzo, F. Fedele, G. Gallego, P.C. Shih, A. Yezzi, Offshore stereo measurements of gravity waves, Coastal Eng. 64 (2012) 127–138.
[11] R. Klette, K. Schlüns, A. Koschan, Three-dimensional Data from Images, Springer-Verlag Singapore Pte. Ltd., Singapore, 1998.
[12] C. Peureux, A. Benetazzo, F. Ardhuin, Note on the directional properties of meter-scale gravity waves, Ocean Sci. 14 (1) (2018) 41.
[13] P.J. Cobelli, A. Maurel, V. Pagneux, P. Petitjeans, Global measurement of water waves by Fourier transform profilometry, Exp. Fluids 46 (6) (2009) 1037.
[14] P. Cobelli, A. Przadka, P. Petitjeans, G. Lagubeau, V. Pagneux, A. Maurel, Different regimes for water wave turbulence, Phys. Rev. Lett. 107 (21) (2011) 214503.
[15] Kinect For Windows Sensor Components and Specifications, Tech. Rep. Elsevier. URL http://msdn.microsoft.com/en-us/library/jj131033.aspx (Online).
[16] K.D. Mankoff, T.A. Russo, The Kinect: A low-cost, high-resolution, short-range 3D camera, Earth Surf. Processes Landforms 38 (9) (2013) 926–936.
[17] M. Viager, Analysis of Kinect for Mobile Robots. Tech. Rep., Technical University of Denmark, Lyngby, 2011.
[18] B. Combes, A. Guibert, E. Memin, D. Heitz, Free-surface flows from Kinect: Feasibility and limits, in: FVR2011, 2011, p. 4.
[19] A. Corbetta, C.m. Lee, R. Benzi, A. Muntean, F. Toschi, Fluctuations around mean walking behaviors in diluted pedestrian flows, Phys. Rev. E 95 (3) (2017) 032316.